

Conductance through analytic constrictions

D. Koudela^{1,2}, A.-M. Uimonen^{1,2}, and H. Häkkinen^{1,2,3}

¹ Nanoscience Center, P.O. Box 35, FIN-40014 University of Jyväskylä, Finland

² Department of Physics, P.O. Box 35, FIN-40014 University of Jyväskylä, Finland

³ Department of Chemistry, P.O. Box 35, FIN-40014 University of Jyväskylä, Finland

Received: date / Revised version: date

Abstract. We study the dependence of the intrinsic conductance of a nanocontact on its shape by using the recursion-transfer-matrix method. Hour-glass, torus, and spherical shapes are defined through analytic potentials, the latter two serving as rough models for ring-like and spherical molecules, respectively. The sensitivity of the conductance to geometric details is analyzed and discussed. Strong resonance effects are found for a spherical contact weakly coupled to electron reservoirs.

PACS. 73.23.Ad Ballistic transport – 73.63.Rt Nanoscale contacts

1 Introduction

Nanocontacts are a research topic of intense current interest, motivated by the drive to reduce the size of integrated circuits [1]. Molecules, molecule-like species and nanoparticles have been considered as natural building blocks for interconnects. Especially Benzene-dithiolate [2, 3, 4, 5, 6, 7, 8, 9, 10, 11, 12, 13, 14, 15, 16, 17, 18, 19, 20, 21, 22] and C₆₀ [23, 24, 25, 26, 27, 28, 29, 30, 31] have been extensively studied.

Gaining detailed knowledge of bias-dependent quantum transport requires high-level ab initio calculations on the coupling of the molecular orbitals between the interconnect and the leads. However, an instructive view of ballistic properties of the contact can be achieved via considering a general quantum mechanical transmission problem through an analytically defined constriction of various shapes. Here we calculated the conductance of a torus connected to jellium electrodes as a crude model for a Benzene-ring and the conductance of two concentric spheres which can be seen as a model for C₆₀. In addition we investigated if two nanoconstrictions in close contact interact with each other.

Among the variety of available methods to calculate quantum transport we have chosen the Recursion-Transfer-Matrix (RTM) method [32, 33]. Compared to the Green's function methods which are widely used for calculating the conductance of nanocontacts the RTM method has the advantage that it needs just a potential as input and uses no atomic orbitals. This feature made it possible to study simple potentials, only determined by geometry where parameters can be changed easily.

This paper is organized as follows: In Sect. 2 we briefly discuss the method. The results are discussed in Sect. 3. First we examine any interference effects when two nanoconstrictions are in close contact. Then we investigate how the conductance of a torus depends on its geometry. Finally we present results for the conductance of the concentric spheres for two cases: in the first case the constriction has cylindrical symmetry and in the second case the symmetry is broken. Sect. 4 concludes the paper.

2 Method

We calculated the conductance using the RTM method [32, 33]. In this method the Schrödinger equation is solved, where the potential is given on a grid and the energy E of the transmitting electron is chosen. As an ansatz for a constriction along the z -direction one expands the wave function into plane waves in the xy -plane

$$\psi_j(\mathbf{r}_\perp, z) = e^{i\mathbf{k}_\perp \cdot \mathbf{r}_\perp} \sum_i \phi_{ij}(z) e^{i\mathbf{G}_\perp^i \cdot \mathbf{r}_\perp} \quad (1)$$

where \mathbf{G}_\perp^i are reciprocal lattice vectors in the xy -plane and for the boundary condition one uses

$$\phi_{ij}^{\text{entr}}(z) = \delta_{ij} e^{ik_z^j z} + r_{ij} e^{-ik_z^i z} \quad (2)$$

$$\phi_{ij}^{\text{exit}}(z) = t_{ij} e^{ik_z^i z} \quad (3)$$

for extremal values of z , where $\phi_{ij}^{\text{entr}}(z)$ denotes the wave function in the entrance and $\phi_{ij}^{\text{exit}}(z)$ denotes the wave function in the exit electrode. The components of the reflexion matrix are denoted by r_{ij} . After the calculation

of the transmission matrix \underline{t} ($(\underline{t})_{ij} = t_{ij}$), one uses the Landauer-Büttiker formula

$$G = \frac{2e^2}{h} \sum_{ij} |t_{ij}|^2 \quad (4)$$

to calculate the conductance G , where G is measured in units of $G_0 = 2e^2/h$. The eigenchannels are the eigenvalues of $\underline{t}^\dagger \underline{t}$ [34].

The convergence of the results was carefully tested with respect to the energy cut-off, the number of grid points and the distance between the grid points. We use atomic units throughout the paper.

3 Results and Discussion

3.1 Two constrictions in close contact

To investigate if two constrictions in close contact interact with each other we calculated the conductance for the following geometry (see Fig. 1):

$$\begin{aligned} V = & V_0 \Theta(R+z) \Theta(R-z) \times \\ & \times \Theta(x^2 + (y + (R + W/2 + d/2))^2 - \\ & - (R + W/2 - \sqrt{R^2 - z^2})^2) \times \\ & \times \Theta(x^2 + (y - (R + W/2 + d/2))^2 - \\ & - (R + W/2 - \sqrt{R^2 - z^2})^2) \end{aligned} \quad (5)$$

We used $V_0 = 0.404$, $R = 5$ and $W = 10$. The distance between the constrictions was varied by varying d . We probed the contact at an energy $E = 0.202$. Our results show that there is no interaction between the two constrictions. Additionally we made calculations using $R = 2$ which are showing no interaction either. Due to the geometrical construction of the constriction it is not possible to calculate distances between the thinnest points of the constriction which are smaller than $2R + W$. Anyway for smaller distances there may be chemical bonding if real atoms are considered.

3.2 Torus connected to electrodes

Another geometry which we studied is a torus. The geometry we used is displayed in Fig. 2 where a cut along the yz -plane is shown. In addition the figure explains all the parameters. So c denotes the radius from the center of the ring to the center of the torus tube. The radius of the latter is called a . The torus is cut at $z = \pm D$ in a plane parallel to the xy -plane to open a pipe for the connection to the electrodes. This distance D also determines the cross-section of the pipe since the pipe is just a prolongation of the hole which is created by the cut. The total length of this pipe is the sum of L and r_0 , where in addition r_0 is the inverse of the curvature of the opening from the pipe to the electrode. For these parameters we have chosen the following values: $a = 4$, $c = 10$, $D = 11$, $L = 4$, $r_0 = 1$, $V_0 = 0.404$ and $E = 0.202$.

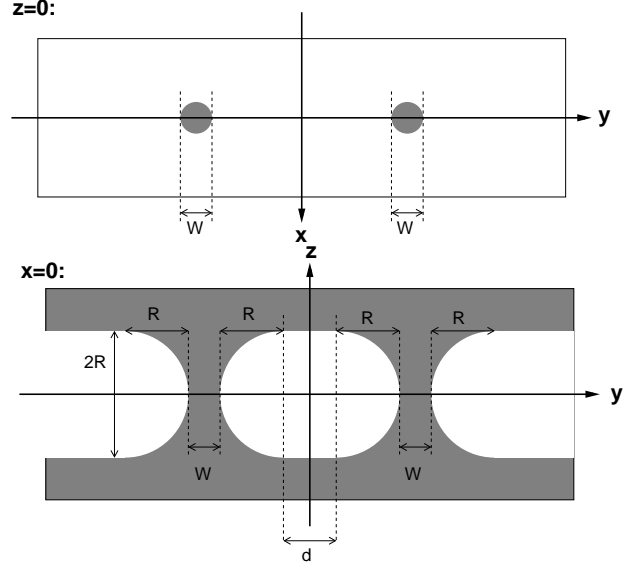


Fig. 1. Geometry of the unit cell. The upper panel shows a cut through the contact perpendicular to the z -axis for $z = 0$. The lower panel shows a cut through the contact perpendicular to the x -axis for $x = 0$. At the white area the potential has the value $V = V_0$ and the grey area denotes zero potential. The electrodes (in which $V = 0$) are located at $z > R$ and $z < -R$.

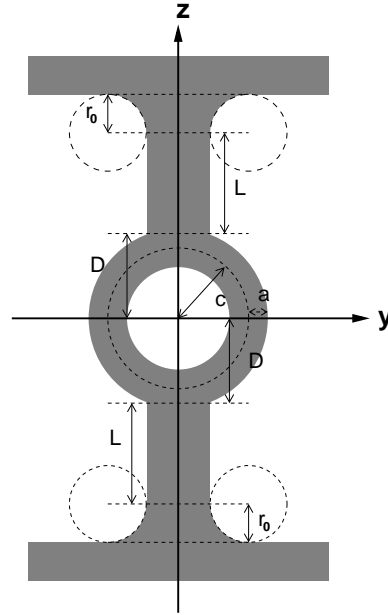


Fig. 2. Geometry of the unit cell at $x = 0$. At the white area the potential has the value $V = V_0$ and the grey area denotes zero potential. The electrodes (in which $V = 0$) are located at $z > D + L + r_0$ and $z < -(D + L + r_0)$.

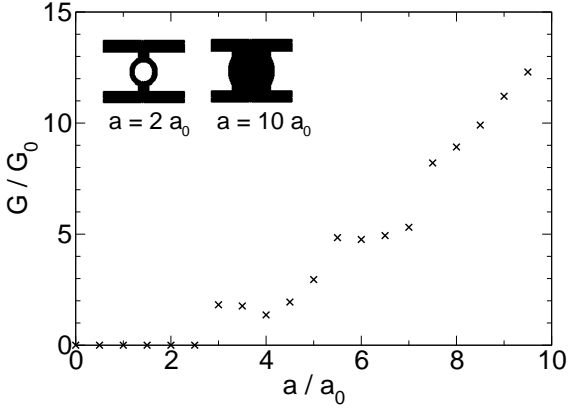


Fig. 3. Conductance versus radius of the tube of the torus a . The other parameters have been chosen to be $c = 10$, $D = 11$, $L = 4$, $r_0 = 1$, $V_0 = 0.404$ and $E = 0.202$. The insets show the geometry of the contact perpendicular to the x -axis for $a = 2$ (left inset) and $a = 10$ (right inset).

To investigate the dependence of the conductance on these geometrical parameters, calculations have been done, where we varied one parameter and left the other parameters constant: Figure 3 displays conductance against the radius a of the tube of the torus. The larger a the larger is the conductance. Increasing a increases also the diameter of the pipes, which connect the torus to the electrodes, since D is kept constant.

One can see conductance steps at $a = 3$, $a = 5.5$ and $a = 7.5$. This can be understood as follows: In the calculation an electronic energy of 0.202 is used. This corresponds to a wavelength λ of 9.9. When a is smaller than about 2.7 then the tube and the pipes are too narrow to support half a wavelength and thus there is no current going through. For $2.7 < a < 5.1$, half a wavelength fits through the constriction and thus we can see the first conductance step. If $5.1 < a < 7.4$, the system can support one wavelength and the conductance jumps up to $G = 5 G_0$. The next conductance step takes place at $a = 7.4$ because from $a = 7.4$ on until $a = 9.9$ the constriction is able to support 1.5 wavelengths. If a is larger than 9.9 two wavelengths are fitting inside the system and so one would expect the next conductance step at $a = 10$.

The dependence of the conductance on D is displayed in Fig. 4. As expected the conductance decreases with a decreasing cross-section of the pipe (increasing D).

Fig. 5 displays the energy-dependence of the conductance for the considered geometry. For energies larger than about 0.1 the system conducts. The increase of the conductance with increasing energy goes stepwise. The second conductance step takes place around $E = 0.3$. At the conductance plateaus the conductance shows oscillations. At the first conductance plateau the conductance oscillates between 1 and $2 G_0$, on the second plateau the conductance takes values between 4 and $5 G_0$.

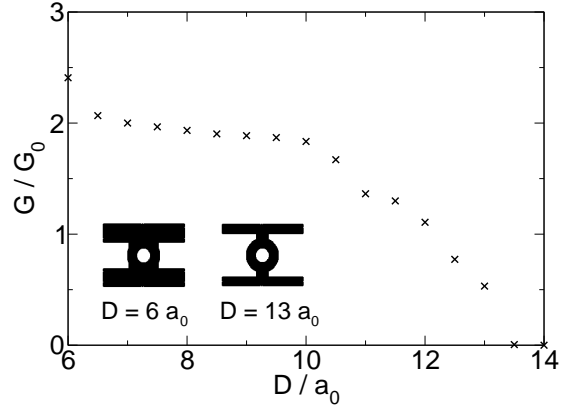


Fig. 4. Conductance versus D , where D is a measure not only where the torus is cut but also for the size of the pipes connecting the torus to the electrodes. The insets show the geometry of the contact perpendicular to the x -axis for $D = 6$ (left inset) and $D = 13$ (right inset). The other parameters have been chosen to be $a = 4$, $c = 10$, $L = 4$, $r_0 = 1$, $V_0 = 0.404$ and $E = 0.202$.

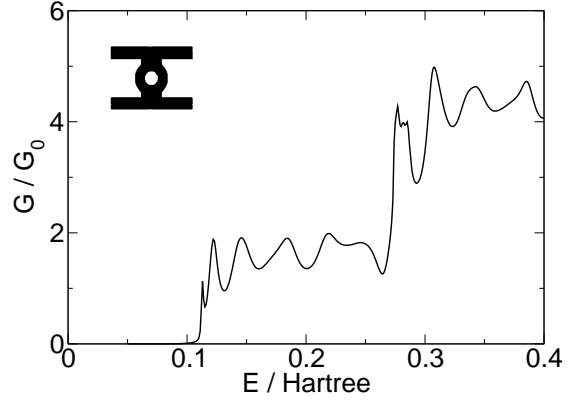


Fig. 5. Conductance versus energy E for a geometry where long pipes connecting the torus to the electrodes. The inset shows the geometry of the contact perpendicular to the x -axis. For this calculation the following parameters have been chosen: $a = 4$, $c = 10$, $D = 11$, $L = 4$, $r_0 = 1$ and $V_0 = 0.404$.

To understand the conductance steps one can argue in a similar way than when varying a (Fig. 3). In this case a is fixed to 4, which means that the wavelength has to be shorter than 16 (8) in order to make half a (one) wavelength fit inside the tube. The connection to the electrodes has an extension of 7.75 in x -direction and an extension of 16.61 in y -direction. Converting these lengths in energy yields that the system should start to be conducting around $E = 0.1$ and the next conductance channel should open around $E = 0.3$.

The oscillations are an effect of the long pipes between the electrodes and the torus. Refs. [35] and [36] calculate

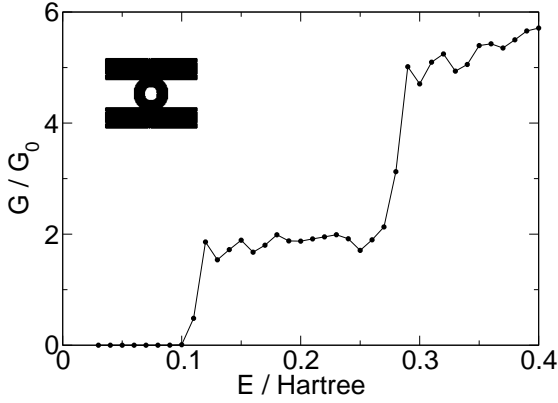


Fig. 6. Conductance versus energy E for a geometry where the torus is almost directly connected to the electrodes. The inset shows the geometry of the contact perpendicular to the x -axis. For this calculation the following parameters have been chosen: $a = 4$, $c = 9$, $D = 10$, $L = 0$, $r_0 = 0.5$ and $V_0 = 0.404$.

narrow pipes and find similar oscillations the longer the pipes.

Figure 6 shows conductance versus energy for another set of parameters. Here the parameters are $a = 4$, $c = 9$, $D = 10$, $L = 0$, $r_0 = 0.5$ and $V_0 = 0.404$. This means that now the total length of each pipe is one order of magnitude smaller than in Fig. 5. The differences in the other parameters are small, which means that the main difference is due to the length of the pipes which connect the torus to the electrodes.

We observe that the conductance steps take place at the same energies than in Fig. 5. This is due to the same size of the tubes. In both cases $a = 4$ and the extension of the pipe connecting the torus to the electrodes in x -direction is in both cases 7.75. Only the extension of these pipes in y -direction is here broader (17.32 instead of 16.61). But this time there are much less oscillations at the plateau with a much smaller amplitude. This supports the theory that the oscillations may be due to the length of the straight pipes.

Though our calculations are only a coarse model, we can nevertheless compare them with experiment. There the conductance of a benzene-1,4,-dithiolate molecule between gold electrodes has been measured [16] and a step-like structure of $G(V)$ has been found. Since $G(E)$ can be seen as an approximation to $G(V)$, our results agree qualitatively with experiment.

3.3 Sphere connected to electrodes

The geometry used for calculating the conductance of a sphere is displayed in Fig. 7. Due to the symmetry cylindrical coordinates have been used where $r = \sqrt{x^2 + y^2}$. At the white area the potential has the value $V = V_0$ and the grey area denotes zero potential. Two concentric spheres with radii R_i (inner sphere) and R_a (outer sphere)

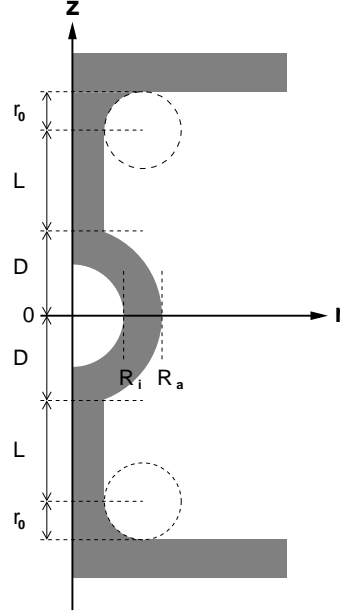


Fig. 7. The geometry used to calculate the conductance through a sphere connected to electrodes. Due to the symmetry cylindrical coordinates have been used. At the white area the potential has the value $V = V_0$ and the grey area denotes zero potential. The electrodes (in which $V = 0$) are located at $z > D + L + r_0$ and $z < -(D + L + r_0)$.

have been used in order to be able to change the thickness of the spherical layer where the electrons are allowed to flow. At a distance D from the center of the spheres in $\pm z$ -direction the sphere is cut parallel to the xy -plane. This cut determines the radius of the pipes which connects the sphere to the upper and lower electrode via

$$r_D = \sqrt{R_a^2 - D^2}. \quad (6)$$

The total length of each pipe is $L + r_0$ where the inverse of r_0 is denoting the curvature of the opening from the pipe to the electrode.

The first panel of Fig. 8 shows the conductance plotted against energy for a sphere which is weakly coupled to the electrodes. In this case "weak coupling" means that there is only a small connection between the sphere and the electrodes. The parameters used in this plot are $R_i = 1.7$ and $R_a = 7.7$ for the radii of the concentric spheres, $D = 7.6$, $L = 0.0$ and $r_0 = 0.5$. Thus there is only a small hole of radius $r_D = 1.2$ connecting the sphere to the electrodes.

For conduction this small hole must be able to contain at least half a wavelength. Using

$$E = \frac{2\pi^2}{\lambda^2} \quad (7)$$

for conversion between wavelength and energy, the system should start to conduct at 0.86. This energy is out of the range displayed in Fig. 8. But what is seen in Fig. 8 are resonances at special energies. These resonances display the eigenstates of the sphere.

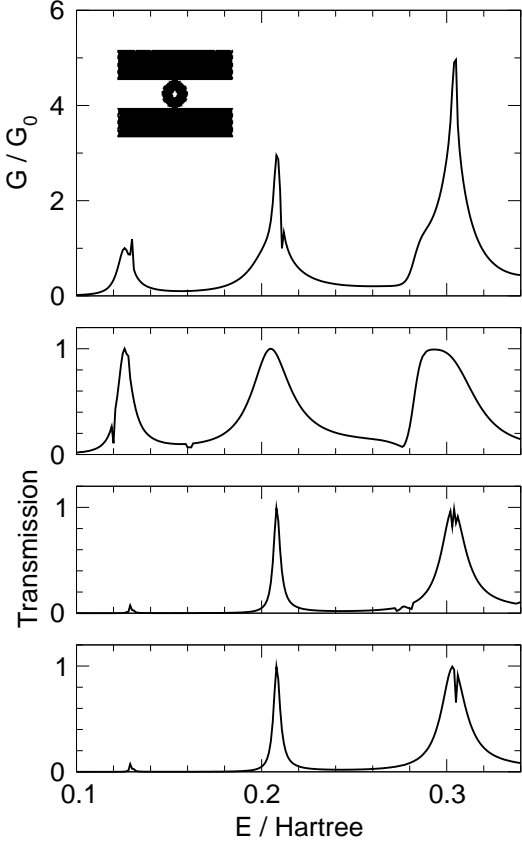


Fig. 8. Top panel: Conductance versus energy for a sphere which is weakly coupled to the electrodes. The three lower panels show the first three eigenchannels. A cut of the potential along the yz -plane is shown in the inset. The parameters used are $R_i = 1.7$ and $R_a = 7.7$, $D = 7.6$, $L = 0.0$ and $r_0 = 0.5$.

The three lower panels of Fig. 8 show the first three eigenchannels of the eigenchannel analysis for the geometry used in Fig. 8. The first channel is non-degenerate but the second and third eigenchannels are degenerate due to the cylindrical symmetry of the constriction.

A different geometry has been used to calculate the conductance versus energy curve shown in the first panel of Fig. 9. Here $R_i = 3.7$, $R_a = 9.7$, $D = 8.6$, $L = 0.0$ and $r_0 = 1.0$. Now $r_D = 4.5$ and using the same argumentation than above one expects that the system conducts for energies larger than 0.06. Fig. 9 confirms our prediction: around $E = 0.06$ the conductance jumps from 0 G_0 to 1 G_0 . With increasing energy the conductance increases but sharp peaks are superpositioned on this increasing conductance. These sharp peaks again display the eigenstates of the sphere. An eigenchannel analysis has been made and the first three eigenchannels are displayed in the lower panels of Fig. 9. The first eigenchannel opens at 0.06 and stays open for higher energies showing some oscillations. The second and the third one are degenerate and are showing some resonances before they open around an energy of 0.2.

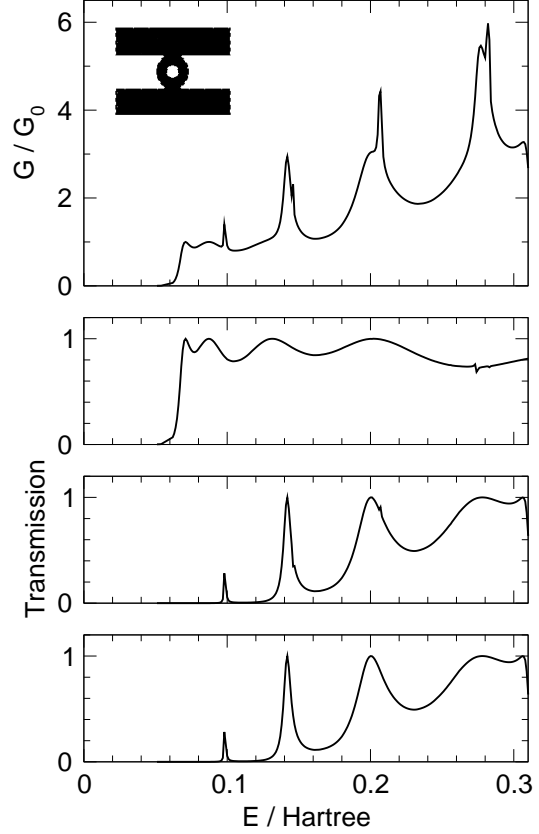


Fig. 9. Top panel: Conductance versus energy for a sphere which is strongly coupled to the electrodes. The three lower panels show the first three eigenchannels. A cut of the potential along the yz -plane is shown in the inset. Geometrical parameters used are $R_i = 3.7$, $R_a = 9.7$, $D = 8.6$, $L = 0.0$ and $r_0 = 1.0$.

The geometries used for obtaining the results in Fig. 8 and Fig. 9 have almost no pipe, the spheres touch more or less directly the electrodes. What changes if the connection to the electrodes is made by long pipes? Fig. 10 shows results obtained for a geometry where all parameters are the same than in Fig. 9 except L . This time $L = 5.0$ is used instead of $L = 0.0$. Now the picture looks much more complex. $G(E)$ (first panel) shows resonances and antiresonances superposing a "background" conductance. The complexity may arise due to the much more complex geometry since every change of geometry (from electrode to pipe, from pipe to sphere and so on) gives rise to reflections. The three lower panels of Fig. 10 show the first three eigenchannels of which two are degenerate. This time the second and third eigenchannel open at an energy of about 0.24. The opening of these two channels can be seen in the first panel of Fig. 10 when the average conductance rises above one conductance quantum.

One can make a qualitative comparison to experiments where the conductance of a C_{60} -molecule has been mea-

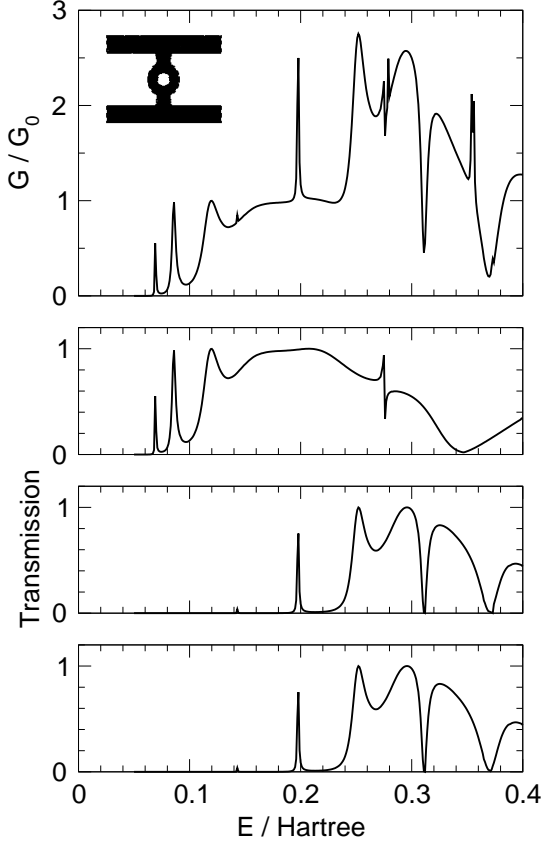


Fig. 10. Top panel: Conductance versus energy for a sphere which is strongly coupled through long pipes to the electrodes. The three lower panels show the first three eigenchannels. A cut of the potential along the yz -plane is shown in the inset. Geometrical parameters used are $R_i = 3.7$, $R_a = 9.7$, $D = 8.6$, $L = 5.0$ and $r_0 = 1.0$.

sured [30]. In these measurements a peaked structure of the conductance has been found as well.

3.4 Sphere connected asymmetrically to the electrodes

Until now cylindrical symmetry has been assumed for the constriction. In addition all constrictions had a mirror plane in the xy -plane. How does it affect the conductance if these symmetries are broken?

To answer these questions calculations have been done where one pipe was shifted away from the z -axis, where y_p denotes the distance from the z -axis and $x_p = 0$ without loss of generality. Fig. 11 shows a cut of the geometry along the yz -plane.

Fig. 12 shows conductance versus y_p . The other parameters were chosen to be $R_a = 10$, $R_i = 5$, $P = 11$, $L = 2$, $D = 8$, $r_p = 3$, $r_0 = 2$, $V_0 = 0.404$, $E = 0.202$. If the upper pipe is situated at the z -axis ($y_p = 0$), the conductance is about $0.82 G_0$. If the upper pipe is shifted away from the z -axis, the conductance increases until it reaches a maximum at $y_p = 2$. There the conductance is

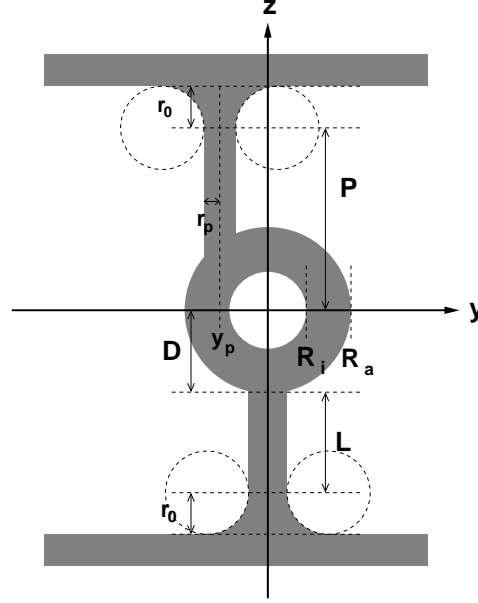


Fig. 11. The geometry used to calculate the conductance through a sphere connected asymmetrically to electrodes. At the white area the potential has the value $V = V_0$ and the grey area denotes zero potential. The electrodes (in which $V = 0$) are located at $z > P + r_0$ and $z < -(D + L + r_0)$.

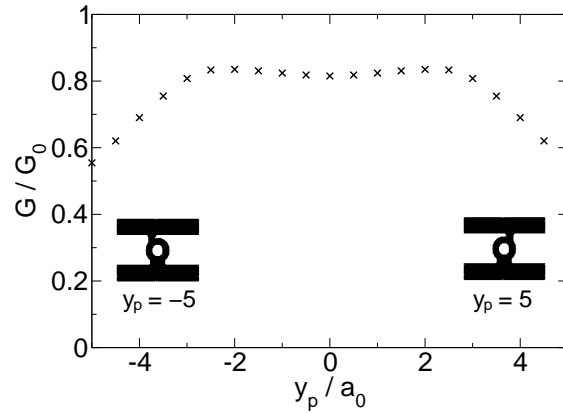


Fig. 12. Conductance versus y_p . The other parameters take the following values: $R_a = 10$, $R_i = 5$, $P = 11$, $L = 2$, $D = 8$, $r_p = 3$, $r_0 = 2$, $V_0 = 0.404$, $E = 0.202$.

$0.84 G_0$. $y_p = 2$ is special in that way, that at this geometry the outer edge of the pipe has the same value of the y -coordinate than the surface of the inner sphere. If the distance of the upper pipe to the z -axis is increased further, the conductance decreases.

4 Conclusions

We calculated the conductance of nanocontacts with different geometries using the recursion-transfer-matrix method. The calculated geometries are two constrictions in close

contact, a torus and two concentric spheres. Our results show that geometry matters. It is not only the diameter of the smallest part of the constriction, which determines the conductance. Furthermore small changes in the geometry can have a large impact on conductance.

For the case of two constrictions in close contact we found, that they do not interact with each other.

In the case of the torus we found a steplike behaviour of the conductance. Each time when there fits half a wavelength more inside the tube by either increasing the radius of the tube or the energy of the electrons there is a conductance-step.

For the sphere a discrete set of energies – its eigenstates – is obtained if the coupling to the electrodes is weak. In the case of strong coupling the resonances remain but the overall behaviour resembles more a step structure.

Moreover the way how the torus or the tube is connected to the electrodes is important for the conductance. Connecting the torus or the sphere with pipes to the electrodes causes more fluctuations in the conductance since the electrons are suffering more reflections. The total conductance is decreased compared to the case with pipes of negligible length.

We would like to thank Matti Manninen for fruitful discussions and the Academy of Finland for financial support.

References

1. M. Brandbyge, K. W. Jacobsen, J. K. Nørskov, Phys. Rev. B **55**, 2637 (1997).
2. K. Hirose, M. Tsukada, Phys. Rev. Lett. **73**, 150 (1994).
3. M. Brandbyge, M. R. Sørensen, and K. W. Jacobsen, Phys. Rev. B **56**, 14956 (1997).
4. O. Lopez-Acevedo, D. Koudela, H. Häkkinen, arXiv:0806.1136.
5. M. A. Reed *et al.*, Science **278**, 252 (1997).
6. H. Park *et al.*, Nature **407**, 57 (2000).
7. N. Agrait, A. L. Yeyati, and J. M. van Ruitenbeek, Phys. Rep. **377**, 81 (2003).
8. D. Q. Andrews, R. Cohen, R. P. Van Duyne, and M. A. Ratner, J. Chem. Phys. **125**, 174718 (2006).
9. H. Basch, R. Cohen, and M. A. Ratner, Nano Lett. **5**, 1668 (2005).
10. C. W. Bauschlicher, J. W. Lawson, A. Ricca, Y. Q. Xue, and M. A. Ratner, Chem. Phys. Lett. **388**, 427 (2004).
11. H. J. Choi, M. L. Cohen, and S. G. Louie, Phys. Rev. B **76**, 155420 (2007).
12. P. Delaney and J. C. Greer, Phys. Rev. Lett. **93**, 036805 (2004).
13. P. A. Derosa and J. M. Seminario, J. Phys. Chem. B **105**, 471 (2001).
14. M. Di Ventura, S. T. Pantelides, and N. D. Lang, Phys. Rev. Lett. **84**, 979 (2000).
15. E. G. Emberly and G. Kirczenow, Phys. Rev. B **58**, 10911 (1998).
16. E. G. Emberly and G. Kirczenow, Phys. Rev. B **64**, 235412 (2001).
17. E. G. Emberly and G. Kirczenow, Phys. Rev. Lett. **91**, 188301 (2003).
18. S. V. Faleev, F. Leonard, D. A. Stewart, and M. van Schilfgaarde, Phys. Rev. B **71**, 195422 (2005).
19. S. H. Ke, H. U. Baranger, and W. T. Yang, J. Am. Chem. Soc. **126**, 15897 (2004).
20. S. H. Ke, H. U. Baranger, and W. T. Yang, J. Chem. Phys. **122**, 074704 (2005).
21. A. K. Maiti, Solid State Commun. **145**, 126 (2008).
22. M. A. Reed, C. Zhou, C. J. Muller, T. P. Burgin, and J. M. Tour, Science **278**, 252 (1997).
23. K. Stokbro, J. Taylor, M. Brandbyge, J. L. Mozos, and P. Ordejon, Computational Materials Science **27**, 151 (2003).
24. K. S. Thygesen and K. W. Jacobsen, Chem. Phys. **319**, 111 (2005).
25. C. Toher and S. Sanvito, Phys. Rev. Lett. **99**, 056801 (2007).
26. J. Ulrich, D. Esrail, W. Pontius, L. Venkataraman, D. Millar, and L. H. Doerrer, J. Phys. Chem. B **110**, 2462 (2006).
27. K. Varga and S. T. Pantelides, Phys. Rev. Lett. **98**, 076804 (2007).
28. J. K. Viljas, F. Pauly, and J. C. Cuevas, Phys. Rev. B **76**, 033403 (2007).
29. S. Alavi, B. Larade, J. Taylor, H. Guo, and T. Seideman, Chem. Phys. **281**, 293 (2002).
30. T. Böhler, A. Edtbauer, and E. Scheer, Phys. Rev. B **76**, 125432 (2007).
31. C. Joachim, J. K. Gimzewski, R. R. Schlittler, and C. Chavy, Phys. Rev. Lett. **74**, 2102 (1995).
32. C. Joachim and J. K. Gimzewski, Chem. Phys. Lett. **265**, 353 (1997).
33. C. C. Kaun and T. Seideman, Phys. Rev. Lett. **94**, 226801 (2005).
34. N. Neel, J. Kroger, L. Limot, T. Frederiksen, M. Brandbyge, and R. Berndt, Phys. Rev. Lett. **98**, 065502 (2007).
35. T. Ono and K. Hirose, Phys. Rev. Lett. **98**, 026804 (2007).
36. H. Park, J. Park, A. K. L. Lim, E. H. Anderson, A. P. Alivisatos, and P. L. McEuen, Nature **407**, 57 (2000).
37. N. Sergueev, A. A. Demkov, and H. Guo, Phys. Rev. B **75**, 233418 (2007).
38. K. Hirose and M. Tsukada, Phys. Rev. Lett. **73**, 150 (1994).
39. M. Brandbyge, K. W. Jacobsen, and J. K. Nørskov, Phys. Rev. B **55**, 2637 (1997).
40. M. Brandbyge, M. R. Sørensen, and K. W. Jacobsen, Phys. Rev. B **56**, 14956 (1997).
41. A. Szafer and A. D. Stone, Phys. Rev. Lett. **62**, 300 (1989).

36. D. van der Marel and E. G. Haanappel, Phys. Rev. B **39**, 7811 (1989).